TITLE PAGE

EX VIVO EXPANSION POTENTIAL OF HEMATOPOIETIC STEM CELLS: A RARE PROPERTY ONLY PARTIALLY PREDICTED BY PHENOTYPE

Qinyu Zhang[1], Anna Konturek-Ciesla[1], Ouyang Yuan[1], David Bryder[1]

[1]Division of Molecular Hematology, Department of Laboratory Medicine, Lund Stem Cell Center, Faculty of Medical, Lund University, 221 84 Lund, Sweden.

Corresponding author:
David Bryder, DMH, BMC B12, Lund University, 221 84 Lund, Sweden +46706423951, 223 951, David.Bryder@med.lu.se

Manuscript information:
Text word count: 7962
Abstract word count: 193
Number of figures: 5
Number of references: 46
Supplemental data: 4 supplemental figures, 9 supplemental tables

Running title: HSC expansion *in vitro*

ABSTRACT

Hematopoietic stem cells (HSCs) reside at the apex of hematopoiesis, can maintain this function for life, and are the functional units in clinical bone marrow transplantation. Limitations in HSC numbers not only restricts their clinical use but also several embodiments of experimental research. Recently, a highly defined *ex vivo* culture system was shown to support several hundredfold expansion of functional *in vivo* HSC activity. Here, we further explored this system. Over a 3-week culture period, only 0.1% of initially seeded HSCs retained their original phenotype, which contained virtually all functional long-term HSC activity in cultures. Despite this low frequency, net HSC expansions were large due to the extensive proliferation in cultures. Limited numbers of expanded HSCs allowed for long-term multilineage engraftment of unconditioned hosts, with expanded HSCs rapidly returning to quiescence in this *in vivo* setting. The *ex vivo* differentiated progeny from candidate HSCs was rich in progenitor cell activity and allowed for radioprotection from even single cultured HSCs. Finally, clonal barcoding and competitive repopulation experiments demonstrated that successful HSC expansion emanated from rare HSC clones that was only partially predicted by phenotype, underscoring the large impact of cellular heterogeneity for HSC biology.

INTRODUCTION

Rare hematopoietic stem cells (HSCs) are the functional units in bone marrow transplantation (BMT) via their ability for multilineage differentiation and long-term self-renewal (Konturek-Ciesla and Bryder, 2022). These properties also position HSCs as the preferred targets for gene therapy/gene editing approaches aimed to cure inherited blood cell disorders. However, restrictions in HSC numbers from limited donor sources, the requirement of harsh host conditioning to permit HSC engraftment and the obstacles to genetically manipulate HSCs with retained functional properties constitute barriers to a wider use of BMT/gene therapy (Walasek et al., 2012).

In the absence of reliable models to assess multilineage differentiation and self-renewal of human HSCs, the mouse remains a preferred model system for experimental HSC biology. Most, if not all, of the limitations with human BMT applies also to the murine system, and have included an inability to effectively expand HSC numbers *in vitro* (Walasek et al., 2012). The scarcity of HSCs remains an obstacle also beyond BMT, for instance in gene-editing or small molecule screens aimed at identifying critical regulators of HSC function.

Recently, culture conditions that better support maintenance and expansion of murine HSCs *ex vivo* were reported (Wilkinson et al., 2019). In this breakthrough approach, purified HSCs could be maintained and expanded in a polyvinyl alcohol (PVA)-based media on fibronectin-coated plates for over a month, with the output of functional HSCs unequivocally validated by BMT. However, expansion of *in vivo* HSC activity over a 28 day period (estimated to 236-899-fold) was not on par with the total cell expansion from candidate HSCs (approximately 10^4-fold), demonstrating that vast amounts of differentiated progeny were generated along with self-renewing HSC divisions (Wilkinson et al., 2019). In further support of this, with the caveat that HSCs might change some phenotypes in culture (Zhang and Lodish, 2005), candidate HSCs by phenotype represented a minor portion of the cells at the end-point of culturing (Wilkinson et al., 2019). While to some extent complicating assessments of HSC expansion, differentiation in an *in vitro* context might also be beneficial. For instance, although stringently purified HSCs have the capacity to sustain hematopoiesis for life following BMT, the most primitive HSCs are not sufficient to provide hematopoietic rescue from the immediate consequences of host conditioning (Nakauchi et al., 1999). For this, progenitors that can more rapidly supply the host with erythrocytes and platelets are needed (Na Nakorn et al., 2002; Yang et al., 2005). To what extent the

PVA system can generate fully radioprotective grafts from HSCs is to our knowledge unknown.

When transplanted into lethally irradiated recipients, functional *in vivo* HSC activity is determined by both quantitative and qualitative monitoring of the fate of candidate HSCs (Purton and Scadden, 2007). Typically, this is assessed using systems where candidate HSCs and their progeny can be distinguished from the host cells and a known amount of competitor cells, with the congenic CD45.1/CD45.2 system prevailing. By comparing the mature progeny of the HSC graft to the portion of competitor-derived cells, the repopulating activity of the candidate graft can be determined (Harrison et al., 1993). However, although the competitive repopulation assay (CRA) represents a mainstay in experimental HSC biology, it associates with shortcomings that are often neglected. First, despite that clinical human BMT aims at transplanting large numbers of HSCs (Barnett et al., 1999; Trebeden-Negre et al., 2010), experimental murine BMT typically use very limited cell numbers for both the HSC grafts to be evaluated and for the competitor portion. For instance, a dose of 200,000 unfractionated BM cells as competitor cells is estimated to contain only 2 repopulating units (Harrison et al., 1993). While this dose is sufficient to rescue most mice from the hematological consequences of lethal irradiation (Purton and Scadden, 2007), its low HSC content is a cause for variation. Relatedly, HSCs in recipients of limited transplants behave differently compared to recipients receiving grafts richer in HSCs (Sawen et al., 2016). Secondly, the CRA is from a quantitative perspective a rather blunt assay, with sigmoidal rather than linear characteristics (Harrison et al., 1993). This feature strongly limits the boundaries of the effects that can be measured. Thirdly, in its original form, the CRA assesses candidate HSC activity based on overall test cell chimerism, which might reflect poorly on the HSC activity given the substantial homeostatic proliferation/maintenance of certain mature hematopoietic cell types (Bryder et al., 2004). Combined, these concerns imply that the traditional use of the CRA risk suffering from high variability among recipients and thus poor (semi)quantitative readouts, and which can strongly influence not only attempts to quantify HSC that have been expanded *in vitro,* but also when approaching HSC enumerations in other settings. At the same time, alternative assays such as limit dilution assays or single-cell transplantation assays are cumbersome, expensive and associated with ethical concerns due to the large numbers of negative mice obtained. Newer developments in DNA barcoding have overcome some of these issues by

allowing for clonal (semi)quantification of many HSC clones in the same host (Lu et al., 2011).

Another factor with the BMT assay is the traditional use of aggressive host conditioning. While this is a part of treatment regimens for leukemic patients, by eradicating malignant cells, the fates of HSCs when comparing transplantation into conditioned hosts to more native hematopoietic contexts are dramatic (Busch and Rodewald, 2016). However, transplantation into unconditioned recipients is inefficient and requires large amount of transplanted HSCs (Brecher et al., 1982). This might be because the sites that can be occupied by transplanted HSCs are few at any given moment and requires sufficient number of HSCs for saturation (Bhattacharya et al., 2009). In fact, it was a key finding in the original work from Wilkinson et al. that *ex vivo* expanded HSCs could permit for successful transplantation into completely un-conditioned hosts (Wilkinson et al., 2019). While not reaching the same levels of chimerism as in conditioned hosts, even low-level HSC chimerism can have strong therapeutic effects as a consequence of the durability of HSCs (Bhattacharya et al., 2006) and many experimental approaches could benefit from avoiding the influence of host conditioning.

Here, we conducted a set of experiments aimed at detailing the *in vitro* PVA-based HSC culture system further. In agreement with the results from Wilkinson et al, substantial *in vitro* self-renewal could be achieved and that necessitated large changes to the standard CRA assay for enumeration. However, initial HSC heterogeneity was a key influencing factor for HSC output even among rigorously purified candidate HSCs. An awareness of this determinism has implications not only for experimental design involving *in vitro* manipulation of HSCs, but also when assessing normal HSC function by BMT.

RESULTS

In vivo HSC activity is retained within cells expressing high levels of EPCR

With the aim to minimize the effect of heterogeneity of the input cells in subsequent experiments, we started to assess the *in vivo* reconstituting activity of candidate HSCs isolated with different phenotypes.

The endothelial protein C receptor (EPCR or PROCR/CD201) was reported to be highly expressed on bone marrow (BM) HSCs (Balazs et al., 2006), while CD41 (ITGA2B) was suggested to be functionally relevant for HSC maintenance and hematopoietic homeostasis (Gekas and Graf, 2013). We therefore isolated 4 subfractions of $Lin^{-}Sca1^{+}cKit^{+}CD150^{+}CD48^{low/-}$ (SLAM LSK) cells based on their expression levels of EPCR and CD41: $EPCR^{high}$, $EPCR^{-}$, $EPCR^{high}CD41^{-}$ and $EPCR^{high}CD41^{+}$ (Fig 1A). 50 cells from each of these fractions were extracted from CD45.1 mice and transplanted together with 500,000 unfractionated whole BM cells from $CD45.2^{+}$ mice into separate lethally irradiated $CD45.2^{+}$ recipients (Fig 1B). Thereafter, chimerism was evaluated in peripheral blood (PB) from short-term (4 weeks) until long-term (16 weeks) after transplantation. At the experimental end-point, we also assessed the chimerism of $EPCR^{+}$ SLAM LSKs in the BM.

Short-term after transplantation, the hematopoietic reconstitution from the three $EPCR^{high}$ fractions was restricted to the myeloid lineages (Fig 1C). By contrast, the majority of these recipients displayed robust long-term multilineage reconstitution (Fig 1C), which was accompanied by equivalent candidate HSC chimerism in the BM (Fig 1D). As for differential CD41 expression, we observed that $EPCR^{high}CD41^{-}$ cells produced more lymphoid cells than the $EPCR^{high}CD41^{+}$ cells at the end-point (Fig S1). However, the candidate HSC chimerism in the BM was very similar in these recipients (Fig 1D). In striking contrast to the *in vivo* HSC activity from the $EPCR^{high}$ fractions, we could only recover test-cell derived myeloid lineage shortly after transplantation from $EPCR^{-}$ cells, with an absence of both long-term PB and candidate BM HSC chimerism (Fig 1C-D).

To further correlate HSC activity with the expression levels of EPCR, we index-sorted single SLAM LSKs co-stained for EPCR, expanded them *ex vivo* for 21 days, and transplanted the progeny of each well to individual lethally irradiated mice. While freshly and stringently isolated HSCs normally fail to rescue mice from lethal irradiation (Nakauchi et al., 1999), we here entertained the idea that culturing of HSCs in addition to inducing self-renewal, would also generate progenitors that could radioprotect the

hosts. If so, survival could be used as a proxy for combined hematopoietic stem and progenitor cell (HSPC) activity.

Correlating back to the index-sorting profiles of the transplanted recipients, we observed that mice receiving progeny from SLAM LSK EPCR higher cells were more efficiently radioprotected (Fig. 1E). Finally, we conducted a similar experiment in which we instead initiated cultures with 50 SLAM LSK cells separated into $EPCR^{high}$ or $EPCR^{lower}$ (but still clearly positive) fractions. Here, mice transplanted with cells expanded from $EPCR^{high}$ cells radioprotected 100% (5/5) of the recipients, while 2 out of 5 animals receiving the progeny of $EPCR^{lower}$ cells survived long-term. As expected, surviving mice displayed exclusive test-cell derived myelopoiesis long-term after transplantation (Fig. 1F).

Taken together, these data demonstrate that HSC activity following transplantation is mainly retained within a population of $EPCR^{high}$ HSCs. Therefore, we operationally defined HSCs as $EPCR^{high}$ SLAM LSK in subsequent work.

Phenotypic heterogeneity of *ex vivo* expanded HSCs

A recently described PVA-dependent cell culture system was reported to efficiently support HSC activity *ex vivo* over several weeks (Wilkinson et al., 2019). However, the functional HSC frequency was not on par with the total amount of cells generated by the end of the culture period, suggesting the generation of also large quantities of more differentiated cells in such cultures (Wilkinson et al., 2019). In a next series of experiments, we therefore detailed the phenotype of such HSC expansion cultures.

We sorted aliquots of 50 HSCs and cultured the cells *ex vivo* for 14-21 days, after which cells from each aliquot were subjected to multicolour phenotyping using a cocktail of lineage markers, Fcer1a, Sca-1, c-kit, CD150, EPCR and CD48 (Fig 2A). We observed an average of 0.5 x 10^6 (14 days) and 13.6 x 10^6 cells (21 days) generated from 50 initial HSCs, respectively (Fig 2B). This was accompanied by a significant phenotypic heterogeneity that increased over time (Fig 2C). Entertaining the working hypothesis that HSCs retain their phenotype in culture, we quantified $EPCR^{high}$ SLAM LSKs and similarly observed a decrease in frequency from day 14 to day 21. However, this decrease was counteracted by the overall proliferation in the cultures. Thus, quantification of candidate/phenotypic HSCs translated into an

average HSC expansion of 54-fold (26- to 85-fold) and 291-fold (86- to 1,273-fold) at 14 and 21 days, respectively.

To explore whether other markers could provide additional phenotypic information, we used an *Fgd5* reporter mouse model that was previously suggested to selectively mark primitive HSCs (Gazit et al., 2014). We isolated aliquots of 50 HSCs from Fgd5-ZsGreen mice and cultured them for 21 days, followed by phenotyping. Most if not all of LSK EPCR^{+}CD150^{+} cells were positive for Fgd5 (Fig 2E), demonstrating that Fgd5 expression levels provided little additional information over the cell surface markers used.

Taken together, these results demonstrate that the phenotypic expansion of HSCs using the PVA-based culture system is robust, albeit with parallel generation also of cells not qualifying as HSCs based on phenotype.

The functional HSC activity of *ex vivo* cultured HSCs can be prospectively associated to a minor Lin^{-}Sca^{+}Kit^{+}EPCR^{+}CD150^{+}CD48^{-} fraction

Given the phenotypic heterogeneity in HSC cultures (Fig 2), we wanted to address if it was possible to prospectively isolate HSCs with *in vivo* long-term multilineage repopulating activity from such cultures.

We isolated 500 HSCs from CD45.1^{+} mice and cultured cells *ex vivo* for 21 days. The expanded cells were next stained with antibodies against the same cell surface markers used to isolate the input HSCs, and separated into two equal portions: one portion was kept unfractionated, while three subpopulations: EPCR^{high}CD48$^{low/-}$, EPCR^{high}CD48^{+} and EPCR^{-} were sorted from the other portion. The fractions from each group were mixed with 2.5 x 10^{6} unfractionated whole BM cells from CD45.2^{+} mice and transplanted into five lethally irradiated CD45.2^{+} recipients. Thus, each recipient received cell fractions equivalent to the expansion from 50 HSCs (EE50) together with 500,000 competitor BM cells (Fig 3A). Chimerism was monitored in PB over time and in BM at the experimental end-point.

We observed stable and very high long-term multilineage reconstitution in all recipients transplanted with unfractionated cells. By contrast, we failed to observe significant test-cell derived reconstitution from EPCR^{-} cells (Fig 3B and Fig S2). For EPCR^{high}CD48^{+} cells, we observed very high reconstitution levels in all mice and evaluated lineages short-term after transplantation. However, in these latter recipients,

the donor chimerism dropped considerably over time (Fig 3B and Fig S2). This differed strikingly from recipients of the minor fraction of EPCR^{high}CD48$^{low/-}$ cells, which presented with robust multilineage reconstitution that persisted long-term after transplantation (Fig 3B and Fig S2). While almost no HSC chimerism was observed in recipients of EPCR^{high}CD48^{+}, some amount of chimerism could be recovered for progenitors residing downstream of HSCs in these recipients. This was in striking contrast to recipients of EPCR^{high}CD48$^{low/-}$ cells, in which high-level chimerism was observed for all evaluated progenitor fractions, including HSCs (Fig 3C).

Taken together, these data demonstrate that functional *in vivo* HSC activity following culture is, similar to BM HSCs, exclusively retained within the EPCR^{high}CD48$^{low/-}$ fraction. By contrast, only transient multilineage reconstitution is observed from EPCR^{high}CD48^{+} cells, a phenotypic fraction barely detectable in normal BM. Finally, the fraction of EPCR^{-} cells is devoid of HSC activity, again similar to that observed from such cells when unmanipulated (Fig 1).

Quantification of HSC activity in *ex vivo* expansion cultures

Thus far, we had observed that cultured HSCs presented with a vastly higher reconstitution activity compared to freshly isolated HSCs, which for the most part fell out of range for accurate quantitative enumerations (Fig 1 and Fig 3B). To try to overcome this limitation, we assessed the impact of lowering the amount of input HSCs and enhancing the amount of competitor cells.

We cultured 10 CD45.2^{+} HSCs per well and expanded the cells for 21 days. Cells from each culture (EE10) were then mixed with 2 or 20 million (2M or 20M) competitor CD45.1^{+} BM cells and transplanted into separate lethally irradiated CD45.1^{+} recipients (Fig 4A). In parallel, we included an additional group in which a similar 21-day culture of 50 HSCs was mixed with 10 million unfractionated BM cells and split among 5 lethally irradiated recipients. Our rational for this was to assess the variability among candidate input HSCs, such that while each recipient here also received a theoretical EE10 together with 2 million competitor cells, each recipient in this group received an equal portion of the same input HSCs. We hypothesized this to result in a more similar test-cell derived HSC output in each recipient. Reconstitution was evaluated over time in PB and for candidate BM HSC frequencies at the experimental end-point (Fig 4A).

In mice transplanted with EE10 from replicate cultures, the amount of test-cell derived cells varied extensively among individual recipients. However, robust reconstitution levels could be observed in most of these recipients (Table 1, Fig 4B-C, Fig S3A-B). To quantify the HSC activity of cultured cells in each recipient, we calculated the repopulating units (RUs) (Harrison et al., 1993) for each lineage and for each recipient separately at the experimental end-point. Cells expanded from 10 HSCs displayed an average of 31 (total donor-derived cells, range 1 – 98), 42 (B cells, range 1 – 144), 18 (T cells, range 2 – 46) and 25 (myeloid cells, range 0 – 57) RUs (Table 1). A higher portion of host T cells explain some of these differences, with another influencing factor relating to the initial production of long-lived mature (lymphoid) cells persisting via homeostatic proliferation. The presence of short-lived myeloid cells has been proposed as a better indicator of ongoing HSC activity (Domen et al., 2000), and in agreement with this, we observed a high correlation between the $RU^{myeloid}$ and RUs assessed for phenotypic HSCs in the BM in most recipients (four out of five) at the experimental end-point (Table 1). In recipients receiving fractions from the same culture, we observed a much more consistent HSC activity in between recipients (Table 1, Fig 4B-C), which confirmed our hypothesis that most of the heterogeneity observed in between individual mice was related to an unresolved cellular heterogeneity of input HSCs. Moreover, the RUs per initial HSC were calculated for freshly isolated BM HSCs (Fig 1B, three groups with $EPCR^{high}$ HSCs transplanted) and after 3-week culture (Fig 4A, pooled EE10 + 2M). 461- and 70-fold increase was observed in PB myeloid cells and BM HSCs within recipients transplanted with *ex vivo* expanded cells, respectively, which provided an estimate of the increase of HSC activity following *ex vivo* culturing (Fig S3G).

To extend our findings, we assessed HSC clonality using a lentiviral barcoding approach (Biddy et al., 2018). Here, five aliquots of 1,000 HSCs were maintained for 48 hours culture and thereafter transduced with the barcode library overnight. Following barcode delivery, cells were *ex vivo* expanded for 19 days. Half of the expanded cells from each well were next transplanted into one ‘parental’ recipient respectively, while the other half of the cultures were mixed with each other and each ‘daughter’ recipient receiving 1/5 of the mixed cells (Fig 4D-i). 16 weeks after transplantation, barcodes were extracted from GFP+ BM myeloid cells, which was followed by high-throughput sequencing to enumerate the contribution of the expanded HSC clones.

Following stringent filtering, we retrieved 223 unique barcodes in the five 'parental' recipients. The clone sizes were determined from the read count of the unique barcodes, and demonstrated a highly variable contribution in parental mice (0.1% - 26.0%, Fig 4E-G).

Representation of the same barcode in 'parental' and 'daughter' recipients would demonstrate a shared clonal/HSC origin. Therefore, clones that are more robustly expanded should have a higher chance of reconstituting more 'daughter' recipients. In agreement with this, we observed that clones recovered from more 'daughter' recipients were observed at higher frequency in 'parental' recipients (Fig 4E). Perhaps not surprisingly, such clones presented at higher average clone sizes also in 'daughter' recipients (Fig 4F).

While our first barcode experiments were designed to assess the *in vitro* expansion potential of candidate/input HSCs, a next set of experiments were executed to assess the clonal HSC activity following expansion. For this, HSCs were *ex vivo* expanded for 13 days, provided with barcodes overnight, followed by transplantation into 4 lethally irradiated recipients (Fig 4D-ii). 16 weeks after transplantation, 573 unique barcodes were recovered from BM myeloid cells from these recipients. The median clone sizes of HSCs post-culture (0.33%) was not only significantly smaller than the 'post-labeled' clones (Fig 4G), but the frequency of large clones were also significantly less abundant (Fig 4H).

Finally, we assessed the potential of the PVA culture system to support the *in vivo* activity of fetal liver (FL) HSCs. FL-HSCs display higher HSC activity when compared to adult HSCs (Rebel et al., 1996), but cell culture conditions previously reported to promote some adult HSC activity failed to promote FL-HSC activity (Miller and Eaves, 1997).

We sorted 50 CD45.1$^+$ FL-HSCs, cultured the cells *ex vivo* and analyzed the phenotypes of the expanded cells by FACS. This revealed that FL-HSCs during a 21-day culture period presented with an average 188-fold increase in phenotypic HSCs (Fig S3D). To functionally evaluate *ex vivo* expanded FL-HSCs, 1/5 of the cultured cells (EE10) were mixed with two different doses of unfractionated CD45.2$^+$ competitor BM cells (2 or 20 million) and transplanted into separate recipients (Fig S3C). *Ex vivo* expanded cells from FL-HSCs contributed considerably to multilineage reconstitution (Fig S3E). However, compared to cells expanded from adult BM-HSCs, calculations

of RU demonstrated a 5.7- and 6.6-fold lower reconstitution ability of expanded FL-HSCs within PB myeloid cells and BM HSCs, respectively (Fig S3F-G).

Taken together, these experiments demonstrate robust increases in HSC activity following culture of candidate HSCs, albeit perhaps slightly less for FL-HSCs. However, clonal barcode assessments revealed substantial variation in *ex vivo* expansion potential of even stringently purified candidate HSCs.

Ex vivo expanded HSCs returns to a quiescent state following engraftment in unconditioned recipients

So far, we had investigated the repopulating ability of *ex vivo* expanded HSCs into lethally irradiated recipients, a standard procedure in the field (Konturek-Ciesla and Bryder, 2022). However, irradiation not only eliminates host hematopoietic cells but also damages other tissue structures, causing irreversibly changes to steady state hematopoiesis (Cao et al., 2011). Thus, engraftment into unconditioned recipients might better mimic native *in vivo* hematopoiesis. Successful engraftment in an unconditioned setting requires large numbers of HSCs/HSPCs (Brecher et al., 1982), which reportedly can be accommodated by PVA-cultured HSCs (Wilkinson et al., 2019).

To begin to assess the capacity of *ex vivo* expanded HSCs to engraft unconditioned mice, we transplanted the EE100 CD45.1$^+$ HSCs into lethally irradiated or unconditioned CD45.2$^+$ recipients (Fig S4A). In lethally irradiated hosts, the progeny of cultured cells reconstituted more than 90% of PB cells, with a virtually exclusive contribution of donor cells to the myeloid lineages (Fig S4B). By contrast, the majority of the unconditioned recipients lacked long-term reconstitution (Fig S4B). Given that CD45 mismatching might constitute a sufficient immunological barrier to prevent HSPC reconstitution (van Os et al., 2001), we next conducted similar experiments in which we also transplanted the expanded cells into unconditioned F1 CD45.1$^+$/CD45.2$^+$ hosts (Fig 5A). While we again failed to observe engraftment in CD45.2$^+$ hosts, we could observe clear long-term multilineage engraftment in all CD45-matched hosts (Fig 5B).

In the BM, HSCs exist for the most part in a quiescent state, which contrasts the situation in cultures in which HSCs become activated and forced to proliferate. This prompted us to ask to what extent *ex vivo* expanded HSCs could return to

quiescence following transplantation. For this, we expanded 100 CD45.2$^+$ HSCs and stained the cells with Cell Trace Violet (CTV), an extensively utilized viable cell division tracking dye, prior to transplantation into CD45.1$^+$/CD45.2$^+$ hosts. As a control, we conducted similar experiments with unmanipulated CD45.2$^+$ cKit-enriched BM cells (Fig 5C). As a control for non-dividing cells, splenic CD4$^+$ enriched cells were co-transplanted into each recipient (Fig S4C). Thereafter, we assessed the reconstitution and HSC fates in the recipient mice biweekly for up to 8 weeks post-transplant.

Although the phenotypic HSC contribution in recipients receiving *ex vivo* expanded cells outnumbered the contribution from unmanipulated cells 2 weeks post-transplantation, the levels became comparable later on (4-8 weeks post-transplantation, Fig 5D). Two weeks post-transplantation, recipients from both groups showed high levels of CTV signal, with the majority of donor EPCR$^+$ HSCs having undergone fewer than 3 cell divisions. With time, increasing numbers of HSCs had proliferated within both groups and with similar patterns (Fig 5E-F), although we did note that a slightly higher number of undivided HSCs could be retrieved from *ex vivo* expanded HSCs at all time points (Fig 5E). Finally, we observed that the most quiescent candidate HSCs associated with higher EPCR levels (Fig S4E), again attesting to the usefulness of EPCR as for predicting robust HSC activity.

Taken together, these experiments demonstrate that *ex vivo* expanded HSCs can efficiently engraft immunologically matched hosts without conditioning. Under such conditions, cultured HSCs efficiently return to quiescence.

DISCUSSION

The ability to maintain or even expand human HSCs in culture is a pre-requisite for applications aimed at permanent gene-correction or to improve graft performance from limited donor sources (Wilkinson et al., 2020a). While considerable efforts have aimed at expanding human HSCs, the ability to appropriately assay human HSCs remains a bottleneck (Konturek-Ciesla and Bryder, 2022). Therefore, how advances eventually will translate to clinical human HSC and gene-marking protocols remains for the most part to be determined. Meanwhile, studies using relevant animal models such as the mouse, which allow for rigorous assessments of HSC properties, remain key to understand and functionally detail the fate processes of HSCs.

Although many efforts have aimed to *in vitro* expand murine HSCs, the results have for the most part been disappointing (Wilkinson et al., 2020a). A recent study suggested that the substitution of undefined serum products with the synthetic polymer PVA is one key determinant towards this goal (Wilkinson et al., 2019). Here, we set out to detail this culture system further. We focused on the requirements of candidate input HSCs, the reproducibility of the system, the cellular output and the functional *in vivo* performance of the *in vitro* replicating HSCs. Several observations that we believe are valuable not only for future applications of the PVA culture system, but also for HSC biology in general, emerged from this work.

While the PVA-system can support HSC activity also from less pure or even unfractionated BM cell preparations (Ochi et al., 2021), which we have reproduced (QZ and DB, unpublished observations June 2022), the phenotypic and actual long-term repopulating HSCs (LT-HSCs) in such crude input cell preparations is very low. Thus, while using less defined HSC-containing cell isolates has its own advantages, this makes it difficult to track the fates of candidate HSCs. Apart from many unresponsive non-HSCs that will die, which might possibly render indirect effects on HSCs, a large number of non-HSCs also necessitates larger culture volumes. Given the relatively high costs of cytokines, recombinant fibronectin and other media components, this is unwanted. Therefore, we here consistently initiated cultures with more stringently purified HSCs.

As a starting point, we used HSCs isolated based on a SLAM phenotype (Lin-Sca+Kit+CD48-CD150+), a current standard in the field (Challen et al., 2021). However, and in agreement with previous reports (Kent et al., 2009), we observed that the addition of CD201/EPCR to SLAM defined HSCs could further enrich for LT-HSCs.

This applied both to HSCs isolated directly from the BM, and when assessing HSC repopulating activity following culture. In fact, despite that HSCs change many phenotypes in culture (Zhang and Lodish, 2005), we could establish that the LT-HSC activity following culture was remarkably enriched in the EPCR positive fraction, but also for other phenotypic attributes of unmanipulated LT-HSCs. This included the absence of lineage markers, expression of Sca1, c-kit and CD150, and lack/low expression of CD48. Importantly, such prospectively isolatable HSCs represented only a very minor fraction in cultures (0.6% and 0.1% of 2- and 3-week cultures, respectively). However, the massive overall expansion in cultures nonetheless led to large net expansions of such cells (100- to 1,200-fold).

It was suggested that the quality/HSC content of PVA cultures can be assessed by the presence of cells with a Lin-Sca+Kit+CD150+ phenotype (Wilkinson et al., 2020b). However, our data demonstrate that additional markers such as EPCR and CD48 are needed to better predict the LT-HSC activity both before and after culture. This was in contrast to inclusion of CD41, a marker previously suggested to functionally subdivide the pool of LT-HSCs (Gekas and Graf, 2013). Although some slight differences were observed in the type of offspring generated from freshly isolated CD41 positive or negative HSCs, CD41 status offered little further enrichment/subdivision of functional LT-HSC activity when used in conjunction with other LT-HSC markers (i.e., for SLAM, EPCR, CD48). In cultures, this was the case also when assessing reporter expression of the HSC-associated Fgd5 gene. Thus, while Fgd5 expression enriches for HSC activity of cultured HSCs, it is not exclusive to LT-HSCs in this setting. That said, our studies emphasize that even when trying to approach a stringently purified “homogeneous” LT-HSC fraction such as SLAM EPCR+ HSCs, considerable functionally heterogeneity is exposed when such cells are approached by transplantation.

While our clonal barcoding experiments unequivocally demonstrated HSC self-renewal, the large spectra in expansion potential of individual candidate HSCs was noteworthy. This variation was reduced when assessing HSCs following culture and aligns with the interpretation that those HSCs that expand robustly in cultures exhibit less intraindividual differences. Nonetheless, the demonstrated *in vitro* self-renewal refutes the alternative views in which the culture process would mainly act to enhance the reconstitution capacity of individual HSCs, for instance by altering their homing properties and/or by the conversion of more differentiated progenitors into cells with

LT-HSC activity. That said, perhaps our data can also be taken as support for the view that this (or other) culture systems might not universally support all types of LT-HSCs that has previously been eluded to (Haas et al., 2018). Further support to this notion can be eluded to from our data on fetal liver HSCs, which did not expand better than adult HSCs in the PVA system, despite that FL HSCs repopulate mice more efficiently than adult HSCs when unmanipulated (Rebel et al., 1996). Whether the variation in expansion potential among individual HSCs reflect differences in the intrinsic self-renewal abilities of individual HSCs, with different fate options, remains unknown. In a broader sense, this associates also with the general concept of "self-renewal" and that has recently been highlighted in studies on native hematopoiesis, where distinct but only slowly contributing LT-HSCs co-exist with more active progenitors that can also execute self-renewal divisions (Busch et al., 2015; Sawen et al., 2016; Sun et al., 2014). It appears that many aspects of this structure are re-created in cultures and, as we show, this requires as input the normally very slowly dividing and presumably most primitive LT-HSCs.

While the parallel self-renewal and differentiation in the PVA HSC cultures represent a fundamental difference compared to other *in vitro* stem cell self-renewal systems (e.g., for ES/iPS cells), where preferential self-renewal can be achieved, the differentiation processes of HSCs can be taken advantage of. More specifically, we demonstrate that the generation of large amounts of potent short-term reconstituting progeny can enhance the speed of donor reconstitution and alleviate the effects of myeloablative conditioning. In fact, as we demonstrate, even single candidate HSCs can on occasion generate sufficient HSCs and offspring to both rescue mice from lethal irradiation and provide long-term durable multilineage reconstitution. The parallel self-renewal and differentiation can also be harnessed to approach HSC fate decisions at a molecular level, not the least when combined with analyses at clonal resolution (Weinreb et al., 2020). However, as the expansion of cells with genuine LT-HSC activity is far from unlimited, a shortage of HSCs would by all likelihood remain an obstacle for larger-scale screening efforts such as genome-wide CRISPR screens and larger small molecule screens. That said, more limited/focused screens should be tractable. The ability to efficiently manipulate candidate HSCs in PVA cultures and the seemingly increased HSC homogeneity following culture, should aid such efforts.

The competitive repopulation assay (CRA) (Harrison et al., 1993) has emerged as a standard when evaluating HSC activity *in vivo*. However, during the course of our

work, we encountered several aspects of this assay that are often neglected. First, the reconstitution activity of freshly isolated HSCs transplanted at limited numbers highlighted large variations in between individual transplantation recipients. This has been established previously, for instance in extensive single cell transplantation experiments (Benz et al., 2012; Carrelha et al., 2018; Oguro et al., 2013; Yamamoto et al., 2013; Yamamoto et al., 2018), but prospectively isolated HSCs are routinely considered as a rather homogenous entity. This concern with the CRA has been raised previously (Ema and Nakauchi, 2000), but taking into account not only the repopulating activity but also clonal aspects has not reached wide use, likely because it has been very cumbersome. Emerging barcoding technologies, by which a large number of clones can be evaluated in a single mouse, should make this easier.

A second concern with the CRA highlighted from our work was that the progeny from a relatively small number of cultured candidate LT-HSCs (10-50 cells) vastly outcompeted “standard” doses of competitor cells, making quantification unreliable/impossible. This contrasted results from freshly isolated HSCs transplanted at the doses used as input to cultures. Thus, to try to quantify the LT-HSC content following culture, we exploited the effect of lowering the number of transplanted input HSCs and using higher numbers of competitor cells. Overall, this confirmed that the CRA is relatively linear, even when using very high numbers of competitor cells (up to 20 million). Further homogeneity among transplant recipients could be achieved by pooling the content of multiple cultures, followed by their re-partitioning into the individual recipients of a group. Alternatively, one can of course initiate cultures with more input HSCs, and split the content into multiple recipients. This should be relevant for several embodiments aimed at manipulating HSCs in culture where one wants to avoid extensive variation among recipients.

A final consideration with the CRA relates to the definition of ongoing HSC-activity. We and others have previously established that this is best mirrored by the contribution to myelopoiesis (Domen and Weissman, 2003; Norddahl et al., 2011), which was re-confirmed here. While multilineage capacity is considered a defining feature of LT-HSCs, the assessment of repopulation in individual lineages can differ substantially. For instance, when we assessed cultured EPCR+CD48+ cells (with predominantly transient multilineage activity), we observed prominent long-term T cell contribution but only limited myeloid reconstitution. This should not be confused with the concept of HSC lineage-bias, but rather reflects that the pool of T cells *in vivo* can

be maintained by homeostatic proliferation and thus do not require continuous input from HSCs. This consideration is valid also in the setting of the CRA, where the competitor graft (in the form of unfractionated BM cells) contains a large number of progenitor cells that can rapidly fill up a given (lymphoid) compartment. Thus, as opposed to the more classic CRA, where the overall donor contribution is assessed (Harrison et al., 1993), the contribution to more short-lived lineages reflects better the ongoing HSC activity. Thereby, the contribution to lymphoid lineages serves more as a qualitative parameter for multipotency. In line with this, we have observed that when cultured HSCs are barcoded and assessed long-term, there is a strong correlation between barcodes in BM progenitors and myeloid cells, while the pool of mature B cells often is made up of many clones that cannot be recovered in other lineages (OY and DB, unpublished observations June 2022). This is in agreement with previous viral barcoding studies on HSCs (Lu et al., 2011). Thus, short-lived non-self renewing multipotent progenitors, which are generated in great numbers in culture, can contribute extensive (lymphoid) offspring in the long-term and this should not be mistaken for ongoing HSC activity. Regardless, the robust lymphopoiesis obtained from cultured HSCs should be practically useful in experimental immunology.

In a final set of experiments, we explored the potential of th PVA-system to allow for repopulation of non-conditioned hosts. This concept is based on the suggestion that large numbers of HSCs are needed to saturate those few BM niches available for engraftment (Bhattacharya et al., 2006; Czechowicz et al., 2007). Avoiding toxic myeloablation has apart from evident clinical implications also a precedence in experimental murine HSC biology, where lethal myeloablation enforces vigorous HSC proliferation following transplantation (Sawen et al., 2016) and an HSC contribution to hematopoiesis that differ substantially from native contexts (Busch et al., 2015; Sawen et al., 2016; Sun et al., 2014). While the possibility of cultured HSCs to repopulate non-conditioned hosts was one of the primary findings in the original work from Wilkinson et al. (2019), our initial attempts to repopulate non-conditioned CD45.2+ hosts with CD45.1+ cultured HSCs were for the most part unsuccessful. Searching for potential explanations, we observed that the CD45.1/CD45.2 system is sufficiently disparate to mediate complete long-term graft rejection in the non-conditioned setting, which in hindsight has been eluded to previously (Bhattacharya et al., 2006; van Os et al., 2001; Xu et al., 2004). Thus, by matching hosts for CD45-isoforms, we could successfully achieve a consistent low-level (2-5%) long-term

multilineage chimerism in adult non-myeloablated hosts from the cultured progeny of only 100 candidate HSCs. Intriguingly, despite being activated to proliferate *in vitro*, many candidate HSCs rapidly returned to a quiescent state *in vivo*, with the most dormant HSCs exhibiting the most stringent HSC phenotype (SLAM HSCs bearing high levels of EPCR). Thus, apart from highlighting a unique feature of BM HSC niches to restrain HSC proliferation, we anticipate that this application will permit assessments of HSC function that are not confounded by the strong toxic effects mediated by standard myeloablation. As such, it should complement genetic lineage tracing models aimed at exploring both normal and malignant hematopoiesis in more native/physiological contexts (Busch et al., 2015; Sawen et al., 2016; Sun et al., 2014).

In summary, we here characterized and detailed murine HSCs as they self-renew and differentiate *in vitro*. Although many aspects of the PVA system remain to be explored, a powerful *in vitro* self-renewal system has been a long-sought goal in HSC biology, where HSCs have been notoriously difficult to uphold in an undifferentiated/self-renewal state. The merger of this system with recent advances in transplantation biology, genome engineering and single-cell techniques now holds promise for many exciting discoveries of relevance to both basic and more clinically-oriented hematopoietic research.

MATERIALS AND METHODS

Mice

Adult (8-10-week-old) C57Bl/6N (CD45.2^{+}) female mice were purchased from Taconic. Transgenic Fgd5-ZsGreen-2A-CreERT2 mice (Gazit et al., 2014) (JAX:027789) was a kind gift from Derrick Rossi. Mice were maintained in the animal facilities at the Biomedical Center of Lund University and kept in environment-enriched conditions with 12-hour light-dark cycles and water and food provided *ad libitum*. All experimental procedures were approved by a local ethical committee (reference numbers M186-15 and 16468/2020). All efforts were made to reduce animal number and suffering.

BM transplantation

All mice used as recipients were 8 - 12 weeks of age. For conditioned recipients, mice were lethally irradiated (950 cGy) at least 4 h prior transplantation. The conditioned mice received prophylactic ciprofloxacin (HEXAL, 125 mg/L in drinking water) for 2 weeks beginning on the day of irradiation. All transplantations were performed through intravenous tail vein injection. The amount of transplanted test cells and competitor/support cells is indicated in the results section.

In vitro HSC culture

In vitro HSC cultures were performed using F12-PVA based culture condition as previously reported (Wilkinson et al., 2020). In brief, HSCs (EPCR^{high}CD150^{+}CD48$^{-/low}$ LSKs) were sorted from mice 8 - 12 weeks of age. Culture plates were coated with 100 ng/ml fibronectin (Sigma) for at least 1 hour at 37 °C prior to sorting or splitting. HSCs were sorted into 96-well flat-bottom plate (Thermo Scientific) containing 200 µl F12 media (Gibco) supplemented with 1% insulin–transferrin–selenium–ethanolamine (ITS-X, Gibco), 1% penicillin/streptomycin/glutamine (Gibco), 10 mM HEPES (Gibco), 0.1% PVA (87 - 90%-hydrolysed, Sigma), 10 ng/ml animal-free recombinant mouse SCF (Peprotech) and 100 ng/ml animal-free recombinant mouse TPO (Peprotech). Cells were expanded at 37 °C with 5% CO_2 for up to 21 days. The first media changes were performed 5 days ($\geqslant$ 50 initial HSCs), 10 days (10 initial HSCs) or 15 days (single-cell culture) after initiation of cultures and then every 2 days. In case of lentiviral library transduction pre-culture, the first media change was performed 24 h after transduction and then as above. Cells were split into 2 - 4 wells of 96-well plate after

reaching 80 - 90% confluency. Following 14- and/or 21-day expansion, cellularity was assessed using an Automated Cell Counter (TC20, BioRad) and used for flow cytometry analysis and/or transplantation.

Cell preparation

Mice were euthanized by cervical dislocation followed by the dissection of bones (both right and left tibias, femurs, and pelvis), spleens or, in the case of fetuses, from livers. Bones were crushed using a mortar and pestle and BM cells were collected in ice-cold phosphate-buffered saline (PBS, Gibco) with 1% fetal bovine serum (FBS, Sigma-Aldrich) (FACS buffer), filtered through a 100 µm mesh and washed for 10 min at 400 g. Fetal liver (FL) or spleen cells were brought into single cell suspension by grinding through a 100 µm mesh. BM or FL cells were cKit-enriched by anti-cKit-APCeFluor780 (eBioscience) staining, while spleen cells were CD4-enrihced by anti-CD4-APC-Cy7 staining, followed by incubation with anti-APC conjugated beads (Miltenyi Biotec). Magnetic separation was performed using LS columns, according to manufacturer's instructions (Miltenyi Biotec). cKit-enriched BM or FL cells were washed and stained with fluorescently labeled antibodies later for analysis or sorting. CD4-enriched spleen cells were washed and later labeled with CTV.

As a positive control in *in vivo* cell trace experiments, spleen cells were collected and resuspended in 3 ml FACS buffer. Cell concentration was measured and 10 x 10^6 cells were taken for staining with fluorescently labeled antibodies. Cell counting was performed on a Sysmex KX21N Automated Hematology Analyzer.

For chimerism analysis after transplantation, blood was drawn from tail vein into FACS buffer containing 10 U/ml heparin (Leo). After incubating with same volume of 2% dextran (Sigma) in PBS at 37 °C, the upper phase was collected and erythrocytes were lyzed using an ammonium chloride solution (STEMCELL Technologies) for 3 min at room temperature followed by washing.

For analysis and/or sorting after *ex vivo* expansion, cultured cells were resuspended by pipetting and then collected using cell culture media. An aliquot was taken for cell counting before the cells were washed for 5 min at 400 g. Cells were counted using an Automated Cell Counter (TC20, BioRad).

Flow cytometry analysis and FACS sorting

Through the whole procedure, cells were kept on ice as much as possible and the FACS buffer was kept ice-cold. Staining, analysis and sorting were performed as previously described (Sawen et al., 2016). In brief, after washing, cells were resuspended in Fc-block (1:50, 5 x 10^6 cells/50 µl, InVivoMab) for 10 min to reduce unspecific background staining and then for 20 min with a twice concentrated antibody staining mixture (5 x 10^6 cells/50 µl, Supplemental table 1 - 8) at 4 °C in dark. In case biotinylated lineage markers were included in the antibody mix, a secondary staining with streptavidin BV605 was performed for 20 min (1:400, 5 x 10^6 cells/100 µl, Sony) at 4 °C in dark. After a final centrifugation step, the cells were resuspended in FACS buffer containing propidium iodide (1:1000, Invitrogen) for discrimination between viable and dead cells.

All FACS experiments were performed at the Lund Stem Cell Center FACS Core Facility (Lund University) on Aria III and Fortessa X20 instruments (BD). Bulk populations were sorted using a 70-micron nozzle, 0.32.0 precision mask, and flow rate of 2 - 3K events/s. HSCs for single cell culture were index sorted. FACS analysis was performed using FlowJo version 10.8.0 (Tree Star Inc.).

Assessment of HSC heterogeneity via barcodes

Lentiviral barcode libraries were purchased from AddGene (No. 115645 and No. 83993) and amplified according to instructions at Addgene. AddGene 83993 is a Crispri gRNA library that was repurposed here for the purpose of lentiviral barcoding (e.g. no Cas9 was co-expressed). These libraries were kind gifts from Samantha Morris and Jonathan Weissman.

For pre-culture labelling, five wells containing 1000 CD45.1$^+$ HSCs each were sorted and cultured for 48 h. Cells were then transduced with the AddGene 115645 library overnight with approximately 35% transduction efficiency, which was followed by regular culture procedures. After 19 days, expanded cells were collected from each initial wells separately. Half of the expanded cells were transplanted into individual ‘parental’ CD45.2$^+$ recipients and the rest were mixed together and transplanted into five ‘daughter’ CD45.2$^+$ recipients. Each ‘parental’ or ‘daughter’ recipient received an estimated expansion equivalent to 500 candidate HSCs. For post-culture labelling, 3000 HSCs were sorted from CD45.1$^+$ mice and expanded for 13 days. Thereafter, the cells were transduced with the AddGene 83993 library overnight at an approximate

density of 100,000 cells/well. Half of the cultured and transduced cells were transplanted into 5 CD45.2^{+} WT recipients. Each recipient received an estimated expansion equivalent of 300 candidate HSCs, of which approximately 15% were transduced according to assessments of transduction efficiencies. Barcode labelled cells were collected and analyzed from four recipients. For both pre- and post-culture labeling experiments, recipients were lethally irradiated and provided with 500,000 unfractionated CD45.2+ WBM cells each as support. At the experimental end points (17 – 18 weeks after transplantation), barcode labelled BM myeloid cells were sorted into 200 µl RNA lysis buffer (Norgen Biotek Corp) ("pre-culture" barcoding) or pelleted for genomic DNA extraction ("post-culture" barcoding) and proceeded to library preparation and sequencing analysis.

RNA was isolated according to the protocol of Single Cell RNA Purificiation Kit (Norgen Biotek Corp) and cDNA were synthesis using qScript cDNA SuperMix (Quantabio). Genomic DNA was extracted using PureLink Genomic DNA Mini Kit (Invitrogen). The 8- (pre-culture) and 21-base pair (bp) barcodes (post-culture) were amplified by PCR using Q5 High-Fidelity DNA Polymerase (New England Biolabs). Primers used were listed in Supplemental Table 9. Adapters containing index sequences (Supplemental Table 9) were added by PCR for 7 cycles. After each PCR amplification step, the products were cleaned up using SPRIselect beads (Beckman Coulter). Purified libraries were run on Agilent High Sensitivity DNA Kit chip (Agilent Technologies) to verify the expected size distribution, quantified by Qubit dsDNA HS Assay Kit (Thermo Fisher Scientific), and pooled at equimolar concentrations. Pooled libraries were loaded on an Illumina MiSeq Reagent Nano Kit v2 flow cell following protocols for single-end 100-cycle sequencing. Sequencing data were downloaded as FASTQ files that were further assessed with FastQC (v.0.11.2), including read count, base quality across reads, and guanine and cytosine (GC) content per sequence.

After extracting the reads of each barcode, frequency in each recipient was calculated and barcodes with a frequency less than 0.1% were considered background reads. Barcodes present in more than one 'parental' recipient were excluded from analysis (7 % and 2% of barcodes pre- and post-culture, respectively) to avoid the possibility of including HSCs transduced independently with the same barcode. Reads were normalized to 10^6 total reads per recipient followed by statistical analyses.

Cell Trace Violet labelling for *in vivo* HSC proliferation tracing

CD45.2$^+$ cultured cells, cKit-enriched BM cells or CD4-enriched spleen cells were collected, washed and pelleted. Cells were resuspended to a final concentration of 5 x 10^6 cells/ml and labelled with 1 µM CTV (Invitrogen) in PBS for 10 min at 37 °C. The reaction was stopped by adding same volume of ice-cold FACS buffer. After washing again with FACS buffer, CTV labeled EE100 cultured cells or 5 x 10^6 cKit-enriched BM cells were mixed with 2 x 10^6 CTV labeled CD4-enriched spleen cells and transplanted into one CD45.1$^+$/CD45.2$^+$ unconditioned recipients. For analysis, BM cells were cKit-enriched and stained accordingly. CD4 positive spleen cells were collected from the same recipient as a control for positive signal/undivided cells.

Statistical test

Statistical analyses were performed using Microsoft Excel and Graphpad Prism 9. Significance values were calculated by Mann-Whitney tests. Statistical significances are described in figure legends for the relevant graphs. In all legends, n denotes biological replicates.

ACKNOWLEDGMENTS

We acknowledge Dr. Shabnam Kharazi for scientific discussions and technical support, Mr. Yun Sheng for advice on analysis for barcode sequencing and Prof. Hiromitsu Nakauchi and Dr. Adam C. Wilkinson for advice on cell cultures. The work was supported by grants from the Tobias Foundation, the Swedish Cancer Foundation and the Swedish Research Council to D.B. and the Royal Physiographic Society of Lund foundation to Q.Z and A.K-C.

AUTHORSHIP CONTRIBUTIONS

Q.Z. designed the research, performed experiments, analyzed data, and wrote the manuscript; A. K-C and O.Y. performed experiments and analyzed data; D.B. supervised the project, was responsible for funding acquisition, designed the research, analyzed data and wrote the manuscript.

CONFLICT OF INTEREST DISCLOSURES

The authors report no conflict of interest.

REFERENCES

Balazs, A.B., A.J. Fabian, C.T. Esmon, and R.C. Mulligan. 2006. Endothelial protein C receptor (CD201) explicitly identifies hematopoietic stem cells in murine bone marrow. *Blood* 107:2317-2321.

Barnett, D., G. Janossy, A. Lubenko, E. Matutes, A. Newland, and J.T. Reilly. 1999. Guideline for the flow cytometric enumeration of CD34+ haematopoietic stem cells. Prepared by the CD34+ haematopoietic stem cell working party. General Haematology Task Force of the British Committee for Standards in Haematology. *Clin Lab Haematol* 21:301-308.

Benz, C., M.R. Copley, D.G. Kent, S. Wohrer, A. Cortes, N. Aghaeepour, E. Ma, H. Mader, K. Rowe, C. Day, D. Treloar, R.R. Brinkman, and C.J. Eaves. 2012. Hematopoietic stem cell subtypes expand differentially during development and display distinct lymphopoietic programs. *Cell Stem Cell* 10:273-283.

Bhattacharya, D., A. Czechowicz, A.G. Ooi, D.J. Rossi, D. Bryder, and I.L. Weissman. 2009. Niche recycling through division-independent egress of hematopoietic stem cells. *J Exp Med* 206:2837-2850.

Bhattacharya, D., D.J. Rossi, D. Bryder, and I.L. Weissman. 2006. Purified hematopoietic stem cell engraftment of rare niches corrects severe lymphoid deficiencies without host conditioning. *J Exp Med* 203:73-85.

Biddy, B.A., W. Kong, K. Kamimoto, C. Guo, S.E. Waye, T. Sun, and S.A. Morris. 2018. Single-cell mapping of lineage and identity in direct reprogramming. *Nature* 564:219-224.

Brecher, G., J.D. Ansell, H.S. Micklem, J.H. Tjio, and E.P. Cronkite. 1982. Special proliferative sites are not needed for seeding and proliferation of transfused bone marrow cells in normal syngeneic mice. *Proc Natl Acad Sci U S A* 79:5085-5087.

Bryder, D., Y. Sasaki, O.J. Borge, and S.E. Jacobsen. 2004. Deceptive multilineage reconstitution analysis of mice transplanted with hemopoietic stem cells, and implications for assessment of stem cell numbers and lineage potentials. *J Immunol* 172:1548-1552.

Busch, K., K. Klapproth, M. Barile, M. Flossdorf, T. Holland-Letz, S.M. Schlenner, M. Reth, T. Hofer, and H.R. Rodewald. 2015. Fundamental properties of unperturbed haematopoiesis from stem cells in vivo. *Nature* 518:542-546.

Busch, K., and H.R. Rodewald. 2016. Unperturbed vs. post-transplantation hematopoiesis: both in vivo but different. *Curr Opin Hematol* 23:295-303.

Cao, X., X. Wu, D. Frassica, B. Yu, L. Pang, L. Xian, M. Wan, W. Lei, M. Armour, E. Tryggestad, J. Wong, C.Y. Wen, W.W. Lu, and F.J. Frassica. 2011. Irradiation induces bone injury by damaging bone marrow microenvironment for stem cells. *Proc Natl Acad Sci U S A* 108:1609-1614.

Carrelha, J., Y. Meng, L.M. Kettyle, T.C. Luis, R. Norfo, V. Alcolea, H. Boukarabila, F. Grasso, A. Gambardella, A. Grover, K. Hogstrand, A.M. Lord, A. Sanjuan-Pla, P.S. Woll, C. Nerlov, and S.E.W. Jacobsen. 2018. Hierarchically related lineage-restricted fates of multipotent haematopoietic stem cells. *Nature* 554:106-111.

Challen, G.A., E.M. Pietras, N.C. Wallscheid, and R.A.J. Signer. 2021. Simplified murine multipotent progenitor isolation scheme: Establishing a consensus approach for multipotent progenitor identification. *Exp Hematol* 104:55-63.

Czechowicz, A., D. Kraft, I.L. Weissman, and D. Bhattacharya. 2007. Efficient transplantation via antibody-based clearance of hematopoietic stem cell niches. *Science* 318:1296-1299.

Domen, J., S.H. Cheshier, and I.L. Weissman. 2000. The role of apoptosis in the regulation of hematopoietic stem cells: Overexpression of Bcl-2 increases both their number and repopulation potential. *J Exp Med* 191:253-264.

Domen, J., and I.L. Weissman. 2003. Hematopoietic stem cells and other hematopoietic cells show broad resistance to chemotherapeutic agents in vivo when overexpressing bcl-2. *Exp Hematol* 31:631-639.

Ema, H., and H. Nakauchi. 2000. Expansion of hematopoietic stem cells in the developing liver of a mouse embryo. *Blood* 95:2284-2288.

Gazit, R., P.K. Mandal, W. Ebina, A. Ben-Zvi, C. Nombela-Arrieta, L.E. Silberstein, and D.J. Rossi. 2014. Fgd5 identifies hematopoietic stem cells in the murine bone marrow. *J Exp Med* 211:1315-1331.

Gekas, C., and T. Graf. 2013. CD41 expression marks myeloid-biased adult hematopoietic stem cells and increases with age. *Blood* 121:4463-4472.

Haas, S., A. Trumpp, and M.D. Milsom. 2018. Causes and Consequences of Hematopoietic Stem Cell Heterogeneity. *Cell Stem Cell* 22:627-638.

Harrison, D.E., C.T. Jordan, R.K. Zhong, and C.M. Astle. 1993. Primitive hemopoietic stem cells: direct assay of most productive populations by competitive repopulation with simple binomial, correlation and covariance calculations. *Exp Hematol* 21:206-219.

Kent, D.G., M.R. Copley, C. Benz, S. Wohrer, B.J. Dykstra, E. Ma, J. Cheyne, Y. Zhao, M.B. Bowie, Y. Zhao, M. Gasparetto, A. Delaney, C. Smith, M. Marra, and C.J. Eaves. 2009. Prospective isolation and molecular characterization of hematopoietic stem cells with durable self-renewal potential. *Blood* 113:6342-6350.

Konturek-Ciesla, A., and D. Bryder. 2022. Stem Cells, Hematopoiesis and Lineage Tracing: Transplantation-Centric Views and Beyond. *Frontiers in Cell and Developmental Biology* 10:

Lu, R., N.F. Neff, S.R. Quake, and I.L. Weissman. 2011. Tracking single hematopoietic stem cells in vivo using high-throughput sequencing in conjunction with viral genetic barcoding. *Nat Biotechnol* 29:928-933.

Miller, C.L., and C.J. Eaves. 1997. Expansion in vitro of adult murine hematopoietic stem cells with transplantable lympho-myeloid reconstituting ability. *Proc Natl Acad Sci U S A* 94:13648-13653.

Na Nakorn, T., D. Traver, I.L. Weissman, and K. Akashi. 2002. Myeloerythroid-restricted progenitors are sufficient to confer radioprotection and provide the majority of day 8 CFU-S. *J Clin Invest* 109:1579-1585.

Nakauchi, H., H. Takano, H. Ema, and M. Osawa. 1999. Further characterization of CD34-low/negative mouse hematopoietic stem cells. *Ann N Y Acad Sci* 872:57-66; discussion 66-70.

Norddahl, G.L., C.J. Pronk, M. Wahlestedt, G. Sten, J.M. Nygren, A. Ugale, M. Sigvardsson, and D. Bryder. 2011. Accumulating mitochondrial DNA mutations drive premature hematopoietic aging phenotypes distinct from physiological stem cell aging. *Cell Stem Cell* 8:499-510.

Ochi, K., M. Morita, A.C. Wilkinson, A. Iwama, and S. Yamazaki. 2021. Non-conditioned bone marrow chimeric mouse generation using culture-based enrichment of hematopoietic stem and progenitor cells. *Nat Commun* 12:3568.

Oguro, H., L. Ding, and S.J. Morrison. 2013. SLAM family markers resolve functionally distinct subpopulations of hematopoietic stem cells and multipotent progenitors. *Cell Stem Cell* 13:102-116.

Purton, L.E., and D.T. Scadden. 2007. Limiting factors in murine hematopoietic stem cell assays. *Cell Stem Cell* 1:263-270.

Rebel, V.I., C.L. Miller, C.J. Eaves, and P.M. Lansdorp. 1996. The repopulation potential of fetal liver hematopoietic stem cells in mice exceeds that of their liver adult bone marrow counterparts. *Blood* 87:3500-3507.

Sawen, P., S. Lang, P. Mandal, D.J. Rossi, S. Soneji, and D. Bryder. 2016. Mitotic History Reveals Distinct Stem Cell Populations and Their Contributions to Hematopoiesis. *Cell Rep* 14:2809-2818.

Sun, J., A. Ramos, B. Chapman, J.B. Johnnidis, L. Le, Y.J. Ho, A. Klein, O. Hofmann, and F.D. Camargo. 2014. Clonal dynamics of native haematopoiesis. *Nature* 514:322-327.

Trebeden-Negre, H., M. Rosenzwajg, M.L. Tanguy, F. Lefrere, N. Azar, F. Heshmati, R. Belhocine, J.P. Vernant, D. Klatzmann, and F. Norol. 2010. Delayed recovery after autologous peripheral hematopoietic cell transplantation: potential effect of a high number of total nucleated cells in the graft. *Transfusion* 50:2649-2659.

van Os, R., T.M. Sheridan, S. Robinson, D. Drukteinis, J.L. Ferrara, and P.M. Mauch. 2001. Immunogenicity of Ly5 (CD45)-antigens hampers long-term engraftment following minimal conditioning in a murine bone marrow transplantation model. *Stem Cells* 19:80-87.

Walasek, M.A., R. van Os, and G. de Haan. 2012. Hematopoietic stem cell expansion: challenges and opportunities. *Ann N Y Acad Sci* 1266:138-150.

Weinreb, C., A. Rodriguez-Fraticelli, F.D. Camargo, and A.M. Klein. 2020. Lineage tracing on transcriptional landscapes links state to fate during differentiation. *Science* 367:

Wilkinson, A.C., K.J. Igarashi, and H. Nakauchi. 2020a. Haematopoietic stem cell self-renewal in vivo and ex vivo. *Nature reviews. Genetics* 21:541-554.

Wilkinson, A.C., R. Ishida, M. Kikuchi, K. Sudo, M. Morita, R.V. Crisostomo, R. Yamamoto, K.M. Loh, Y. Nakamura, M. Watanabe, H. Nakauchi, and S. Yamazaki. 2019. Long-term ex vivo haematopoietic-stem-cell expansion allows nonconditioned transplantation. *Nature*

Wilkinson, A.C., R. Ishida, H. Nakauchi, and S. Yamazaki. 2020b. Long-term ex vivo expansion of mouse hematopoietic stem cells. *Nat Protoc*

Xu, H., B.G. Exner, P.M. Chilton, C. Schanie, and S.T. Ildstad. 2004. CD45 congenic bone marrow transplantation: evidence for T cell-mediated immunity. *Stem Cells* 22:1039-1048.

Yamamoto, R., Y. Morita, J. Ooehara, S. Hamanaka, M. Onodera, K.L. Rudolph, H. Ema, and H. Nakauchi. 2013. Clonal analysis unveils self-renewing lineage-restricted progenitors generated directly from hematopoietic stem cells. *Cell* 154:1112-1126.

Yamamoto, R., A.C. Wilkinson, J. Ooehara, X. Lan, C.Y. Lai, Y. Nakauchi, J.K. Pritchard, and H. Nakauchi. 2018. Large-Scale Clonal Analysis Resolves Aging of the Mouse Hematopoietic Stem Cell Compartment. *Cell Stem Cell* 22:600-607 e604.

Yang, L., D. Bryder, J. Adolfsson, J. Nygren, R. Mansson, M. Sigvardsson, and S.E. Jacobsen. 2005. Identification of Lin(-)Sca1(+)kit(+)CD34(+)Flt3- short-term hematopoietic stem cells capable of rapidly reconstituting and rescuing myeloablated transplant recipients. *Blood* 105:2717-2723.

Zhang, C.C., and H.F. Lodish. 2005. Murine hematopoietic stem cells change their surface phenotype during ex vivo expansion. *Blood* 105:4314-4320.

TABLES

Table 1. RUs for each lineage in PB and for BM HSCs of each recipient.

Recipients		*PB*	*B cells*	*T cells*	*Myeloid* cells	*BM HSCs*
Individual BM EE10 + 2M	***#1***	6	6	6	4	12
	#2	31	35	19	27	75
	#3	21	23	17	35	70
	#4	98	144	46	57	21
	#5	1	1	2	0.03	0.4
Pooled BM EE10 + 2M	***#1***	101	78	173	583	49
	#2	110	84	120	516	82
	#3	87	68	103	248	130
	#4	101	70	149	384	187
	#5	65	127	186	331	112

** 1 RU equals to the reconstitution activity of 1 x10 ^{5} WBM cells.*

SUPPLEMENTARY TABLES

Supplemental Table 1. Lineage cocktail (Biotinylated)

Surface marker	Coupled dye	Clone	Dilution	Provider
B220	Biotin	RA3-6B2	1:200	Sony
CD3	Biotin	17A2	1:100	Sony
Gr-1	Biotin	RB6-8C5	1:400	Sony
Nk1.1	Biotin	PK136	1:400	BD
Ter119	Biotin	TER-119	1:400	Sony

Supplemental Table 2. Lineage cocktail (PE-Cy5)

Surface marker	Coupled dye	Clone	Dilution	Provider
B220	PE-Cy5	RA3-6B2	1:200	Sony
CD3	PE-Cy5	145-2C11	1:4 00	Sony
Gr-1	PE-Cy5	RB6-8C5	1:400	Sony
Nk1.1	PE-Cy5	PK136	1:400	Sony
Ter119	PE-Cy5	TER-119	1:400	Sony

Supplemental Table 3. Antibody mixture for BM or FL HSC sorting

Surface marker	Coupled dye	Clone	Dilution	Provider
Lineage cocktail	As outlined in Table 2.			
CD48	FITC	HM48-1	1:200	Sony
CD150	PE-Cy7	TC15-12F12.2	1:200	Sony
CD201	PE	RCR-16	1:200	Sony
Sca1	PB	E13-161.7	1:200	BioLegend

* CD41-PerCP-eFluor710 (1:100, Clone eBioMWReg30, eBioscience Cat. #46-0411-82) was included if mentioned in the results.

Supplemental Table 4. Antibody mixture for HSC culture analysis and sorting

Surface marker	Coupled dye	Clone	Dilution	Provider
Lineage cocktail	As outlined in Table 3.			
CD48	AF700	HM48-1	1:100	Sony
CD150	PE-Cy7	TC15-12F12.2	1:200	Sony
CD201	PE	RCR-16	1:200	Sony
cKit	APCeFluor780	2B8	1:100	eBioscience
Fcer1a	FITC	MAR-1	1:200	eBioscience
Sca1	PB	E13-161.7	1:200	BioLegend

* In case of analysis of expansion from Fgd5-ZsGreen labeled HSCs, Fcer1a-FITC was excluded.

Supplemental Table 5. Antibody mixture for PB chimerism analysis

Surface marker	Coupled dye	Clone	Dilution	Provider
CD3	AF700	17A2	1:200	Sony
CD11b	APC	M1/70	1:200	Sony
CD19	PE-Cy7	6D5	1:400	Sony
CD45.1	BV650	A20	1:100	Sony
CD45.2	BV785	104	1:100	Sony
Gr-1	PE	RB6-8C5	1:400	Sony
Nk1.1	PB	PK136	1:200	Sony
Ter119	PerCP-Cy5.5	TER-119	1:200	Sony

Supplemental Table 6. Antibody mixture for BM HSC chimerism analysis

Surface marker	Coupled dye	Clone	Dilution	Provider
Lineage cocktail	As outlined in Table 3.			
CD45.1	BV650	A20	1:100	Sony
CD45.2	BV785	104	1:100	Sony
CD48	AF700	HM48-1	1:100	Sony
CD150	PE-Cy7	TC15-12F12.2	1:200	Sony
CD201	PE	RCR-16	1:200	Sony
cKit	APCeFluor780	2B8	1:100	eBioscience
Sca1	PB	E13-161.7	1:200	BioLegend

Supplemental Table 7. Antibody mixture for BM CTV analysis

Surface marker	Coupled dye	Clone	Dilution	Provider
Lineage cocktail	As outlined in Table 3.			
CD45.1	BV650	A20	1:100	Sony
CD45.2	BV785	104	1:100	Sony
CD48	FITC	HM48-1	1:200	Sony
CD135	PE	A2F10	1:100	Sony
CD150	PE-Cy7	TC15-12F12.2	1:200	Sony
CD201	APC	eBio1560	1:200	eBioscience
Sca1	BV711	D7	1:200	Sony

Supplemental Table 8. Antibody mixture for Spleen CTV analysis

Surface marker	Coupled dye	Clone	Dilution	Provider
CD4	APC-Cy7	GK1.5	1:200	Sony
CD11b	FITC	M1/70	1:400	BD
CD19	PE-Cy7	6D5	1:400	Sony
CD45.1	BV650	A20	1:100	Sony
CD45.2	BV785	104	1:100	Sony
Ter119	PE-Cy5	TER-119	1:400	Sony

Supplemental Table 9. Primer list

Primer pair	Sequence (5' – 3')
Pre-culture Forward	TCGTCGGCAGCGTCAGATGTGTATAAGAGACAGGAAGCTGC GCCTGTCATC
Pre-culture Reverse	GTCTCGTGGGCTCGGAGATGTGTATAAGAGACAGGTGAACC GCATCGAGCTG
Post-culture Forward	TCGTCGGCAGCGTCAGATGTGTATAAGAGACAGTGGAGAAC CACCTTGTTGG
Post-culture Reverse	GTCTCGTGGGCTCGGAGATGTGTATAAGAGACAGTGCATGG CGGTAATACGGT
P5 index N101	AATGATACGGCGACCACCGAGATCTACAC **TAGATCGC** TCGTCGGCAGCGTC
P5 index S502	AATGATACGGCGACCACCGAGATCTACAC **CTCTCTAT** TCGTCGGCAGCGTC
P5 index S503	AATGATACGGCGACCACCGAGATCTACAC **TATCCTCT** TCGTCGGCAGCGTC
P7 index N701	CAAGCAGAAGACGGCATACGAGAT **TCGCCTTA** GTCTCGTGGGCTCGG
P7 index N901	CAAGCAGAAGACGGCATACGAGAT **AACGTGAT** GTCTCGTGGGCTCGG
P7 index N902	CAAGCAGAAGACGGCATACGAGAT **AAACATCG** GTCTCGTGGGCTCGG
P7 index N903	CAAGCAGAAGACGGCATACGAGAT **ATGCCTAA** GTCTCGTGGGCTCGG
P7 index N904	CAAGCAGAAGACGGCATACGAGAT **AGTGGTCA** GTCTCGTGGGCTCGG

FIGURE LEGENDS

Figure 1. EPCR expression within the BM SLAM LSK fraction is a high-confidence predictor of transplantation-associated HSC activity

(A) Expression patterns of EPCR and CD41 within the BM LSK SLAM fraction. Gates depict the assessed cell fractions.

(B) Strategy used to assess the correlation of EPCR and CD41 expression to the *in vivo* HSC activity.

(C) Test-cell derived chimerism 4 and 16 weeks post-transplantation.

(D) Test-cell derived chimerism in BM EPCR^{+} SLAM LSKs.

(E) Correlation between duration of radioprotection and EPCR expression levels. BM LSK SLAM cells were co-stained with EPCR and index-sorted at one cell per well, cultured for 21 days, and the content of each well transplanted to individual recipients (n = 22). Correlation to mortality of individual mice was made by assessing which well was transplanted into which mouse and coupling this to the index-sorting information.

(F) Donor contribution in PB myeloid cells. Mice were transplanted with *ex vivo* expanded cells from either 50 SLAM LSK EPCR^{lower} (n = 5) or 50 SLAM LSK EPCR^{high} cells (n = 5) and assessments made 16 weeks after transplantation.

All data points depict values in individual recipients. Error bars denote SEM. The asterisks indicate significant differences. *, $p < 0.05$; **, $p < 0.01$. In E) a regression line was generated based on an end-point survival of 150 days (the time at which the experiment was terminated).

Figure 2. The phenotypic properties of HSC expansion cultures.

(A) Representative FACS plots of HSCs cultured for 14 days. Cells with an EPCR^{high}CD48$^{low/-}$ phenotype represent phenotypic HSCs.

(B) Overall cell expansion from 50 EPCR^{high} SLAM LSKs after 14- or 21-days of *ex vivo* culture.

(C) Frequency of cells expressing different stem cell markers in *ex vivo* cultures following 14 or 21 days of culture.

(D) Frequency and fold change of phenotypic HSCs (EPCR^{high} SLAM LSKs) in *ex vivo* cultures after 14 or 21 days of culture.

(E) Representative FACS plots of cells expanded 14 days in *ex vivo* cultures using Fgd5-ZsGreen reporter cells. Mean values demonstrate the frequency of Fgd5^{+}Lin^{-}

Fcer1a^{-} or Fgd5^{+}EPCR^{+}CD150^{+}Fcer1a^{-}LSK cells, respectively. Mean ± SEM value was calculated from 15 individual culture initiated from 50 HSCs.

All data points depict values from individual cultures initiated from 50 HSCs. Error bars denote SEM. The asterisks indicate significant differences. **, $p < 0.01$; ***, $p < 0.001$; ****, $p < 0.0001$.

Figure 3. HSC activity can be prospectively isotated from HSC cultures and associates with a minor EPCR^{+} SLAM LSK fraction

(A) Strategy to assess the *in vivo* HSC activity of subfractions from *ex vivo* cultures.

(B) Test-cell derived chimerism in PB myeloid lineages over 24 weeks post-transplantation. Data represent mean values ± SEM (n = 5 for each group).

(C) Test-cell derived chimerism in BM progenitor subsets 24 weeks post-transplantation. Numbers indicate fold differences between the EPCR^{+} CD48$^{-/low}$ and EPCR^{+}CD48^{+} fractions, and data points depict chimerism levels in individual recipients.

Figure 4 Quantification of repopulating activity of HSCs expanded from BM HSCs

(A) Competitive transplantation strategies used to assess the repopulation of *ex vivo* expanded BM-HSCs.

(B) Test-cell derived PB reconstitution 16 weeks post-transplantation. Symbols denote individual mice and means ± SEM.

(C) BM HSCs chimerism 16 weeks post transplantation. Symbols denote individual mice, and means ± SEM.

(D) Barcode approaches used to assess the clonal HSC contribution of *ex vivo* expanded HSCs before (i) or after (ii) *ex vivo* expansion.

(E) Clone sizes of unique barcodes in 'parental' recipients and their appearance in 'daughter' recipients, demonstrating extensive variation in expansion capacity among individual HSCs. Red lines indicate the median clone size in 'parental' recipients.

(F) Clone sizes of unique barcodes detected in BM myeloid cells of 'parental' recipients and their corresponding contribution in 'daughter' recipients. The red line denotes the correlation/linear regression.

(G) Clone sizes in 'parental' recipients transplanted with 'pre-culture' barcoded cells, or in recipients of 'post-culture' barcoded cells. Median clone sizes are shown with interquartile ranges.
(H) Frequency of barcodes and their clone sizes in recipients of pre- or post-cultured barcoded HSCs. BCs, barcodes.
All data points depict values in individual recipients or barcodes. Asterisks indicate significant differences. *, $p < 0.05$; ****, $p < 0.0001$.

Figure 5. Cultured HSCs allow for transplantation into non-conditioned syngeneic recipients.
(A) Strategy to assess the ability of *ex vivo* expanded HSCs to engraft unconditioned recipients. Symbols denote individual mice and means ± SEM.
(B) Test-cell derived PB reconstitution 24 weeks post-transplantation.
(C) Strategy used to assess the *in vivo* proliferation of *ex vivo* expanded HSCs.
(D) BM HSC chimerism 2-8 weeks post transplantation.
(E) Representative CTV label profiles of donor EPCR$^+$ HSCs compared to negative control signal (host EPCR$^+$ HSCs) and positive signal (donor CD4$^+$ spleen cells) at 2 or 8 weeks post-transplantation.
(F) Donor EPCR$^+$ HSCs were evaluated for the number of cell divisions they had undergone through 8 weeks post-transplantation.
All data points depict values in individual recipients.

SUPPLEMENTARY FIGURE LEGENDS

Supplementary Figure 1. The PB lineage output from EPCR^{high}CD41^{-} and EPCR^{high}CD41^{+} cells after transplantation.

(A) The distribution of lymphoid (pooled B and T cells) and myeloid cells out of the test-cell derived reconstitution 16 weeks post-transplantation.

Data points depict values in individual recipients. Error bars denote SEM. The asterisks indicate significant differences. **, $p < 0.01$.

Supplementary Figure 2. B and T cell chimerism in PB after transplantation.

(A) Test-cell derived chimerism in PB B cells, and

(B) Test-cell derived chimerism in PB T cells over 24 weeks post-transplantation.

Data represent mean values (n = 5 per group). Error bars denote SEM.

Supplementary Figure 3. Quantification of HSC activity from cultured BM or FL HSCs

(A) Percentage of test-cell derived cells in PB to each of the assessed lineages 16 weeks post-transplantation. Mice were transplanted with CD45.2^{+} EE10 BM-HSCs together with 2 or 20 million CD45.1^{+} WBM cells.

(B) Test-cell derived chimerism in BM HSCs 16 weeks post transplantation. Mice were transplanted with CD45.2^{+} EE10 BM-HSCs together with 2 or 20 million CD45.1^{+} WBM cells.

(C) Outline of the competitive transplantation strategy to assess the repopulation ability of *ex vivo* expanded FL HSCs.

(D) Phenotypic analysis of *ex vivo* expanded BM-HSCs and FL-HSCs. (i). Overall cell expansion from 50 BM or FL EPCR^{high} SLAM LSKs after 21-days of *ex vivo* culture. (ii). Frequency and fold change of phenotypic HSCs (EPCR^{high} SLAM LSKs) in *ex vivo* cultures after 21 days of culture from BM or FL-HSCs.

(E) Test-cell derived chimerism in PB myeloid cells 16 weeks post transplantation.

(F) Test-derived HSCs chimerism in the BM of the recipients received *ex vivo* expanded cells from BM or FL-HSCs 16 weeks post transplantation.

(G) RUs equivalent to one initial HSC within PB myeloid cells and BM HSCs in the recipients of 50 BM HSCs or *ex vivo* expanded cells from 10 BM or FL-HSCs 16 weeks post transplantation. Fold changes of EE10 BM-HSCs versus 50 fresh BM HSCs or EE10 FL-HSCs are indicated. Median values are shown with interquartile ranges.

All data points depict values in individual recipients or culture wells. Error bars denote SEM. The asterisks indicate significant differences. *, $p < 0.05$; **, $p < 0.01$; ***, $p < 0.001$.

Supplementary Figure 4. The fate of *ex vivo* cultured HSCs following transplantation into unconditioned hosts.

(A) Strategy to assess the repopulation of *ex vivo* expanded HSCs into lethally irradiated or unconditioned recipients.

(B) Test-cell derived PB reconstitution 16 weeks post-transplantation. All data points depict values in individual recipients. Error bars denote SEM.

(C) CTV signal from transplanted $CD4^+$ spleen cells, used to define undivided cells.

(D) Investigation of cell divisions based on CTV signals.

(E) Correlation of EPCR expression levels and the proliferative activity of candidate HSCs.

FIGURES

Figure 1, Zhang et al.

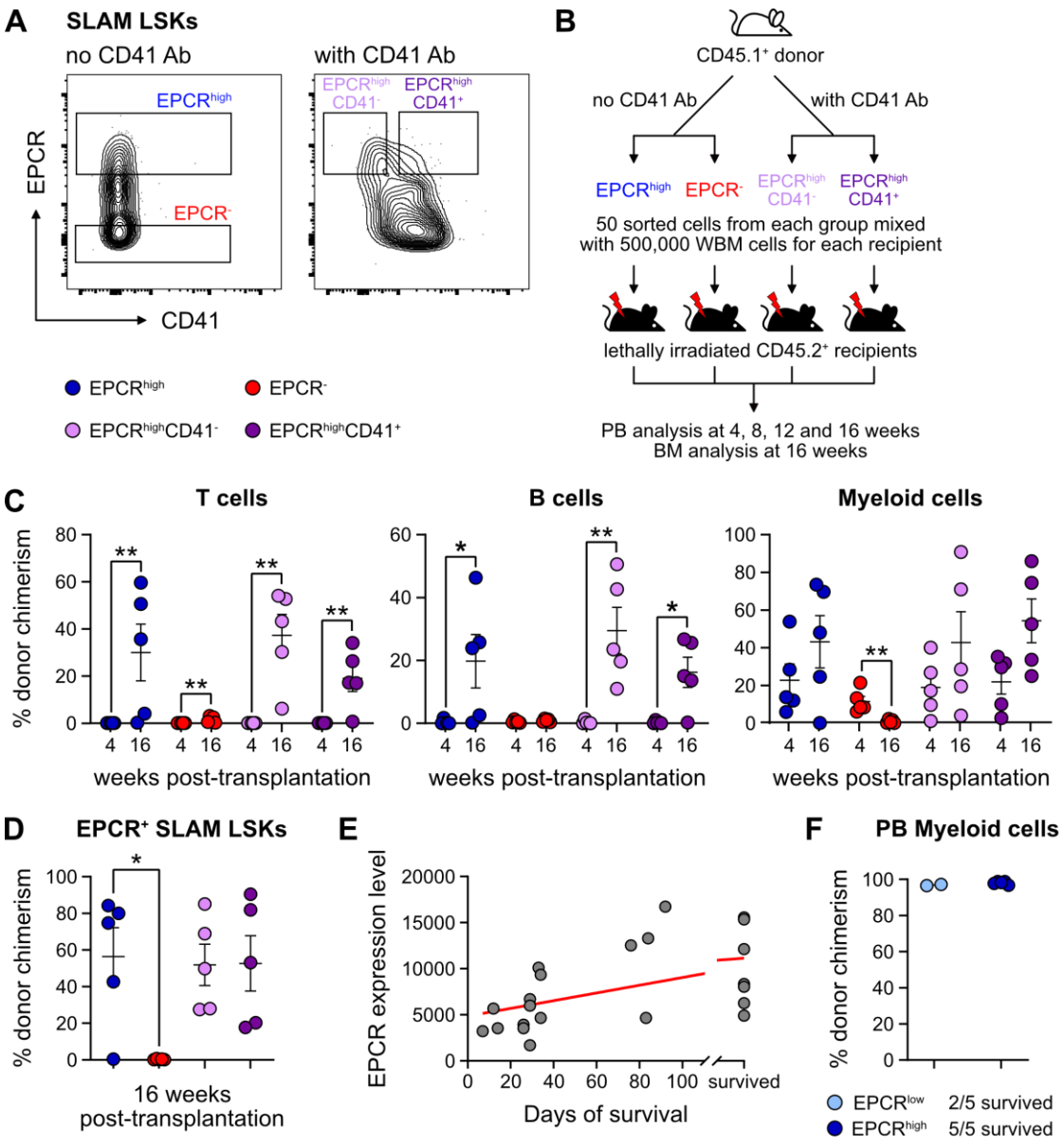

Figure 2, Zhang et al.

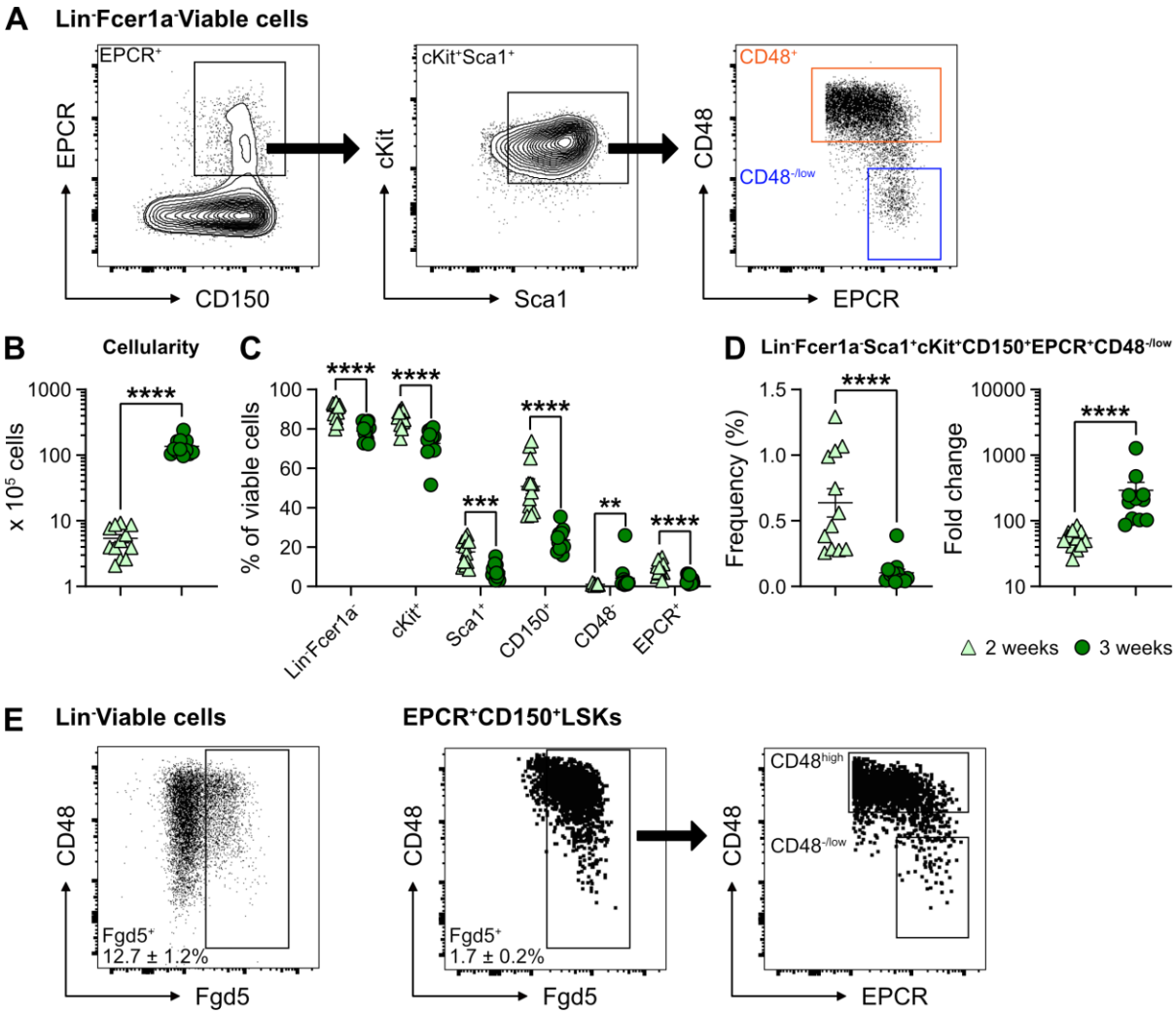

Figure 3, Zhang et al.

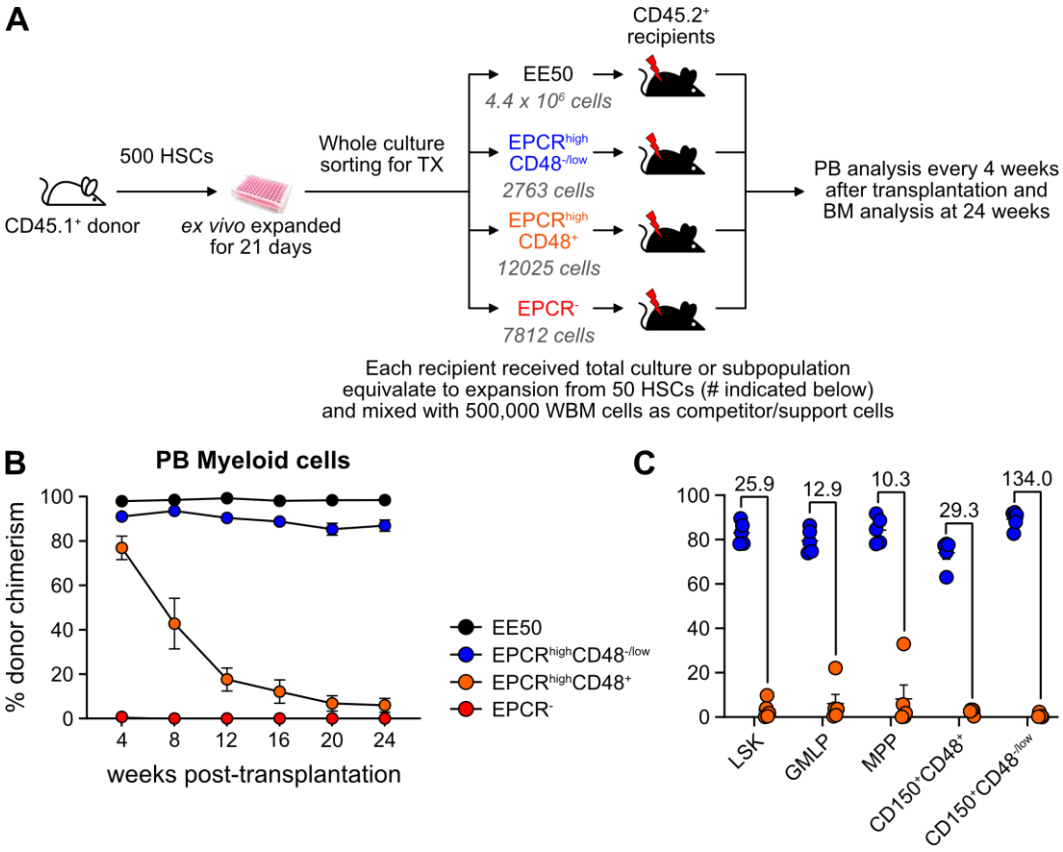

Figure 4, Zhang et al.

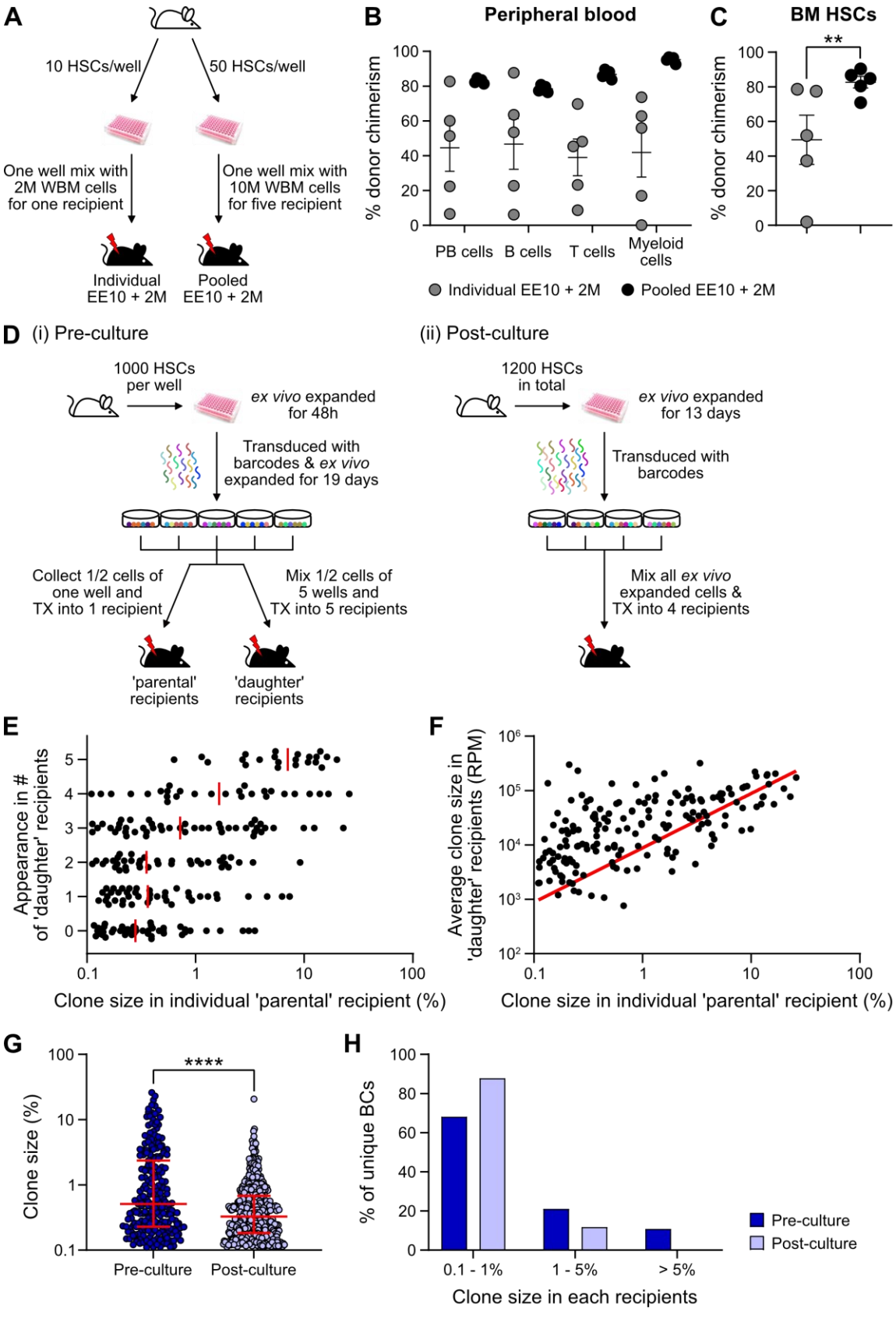

Figure 5, Zhang et al.

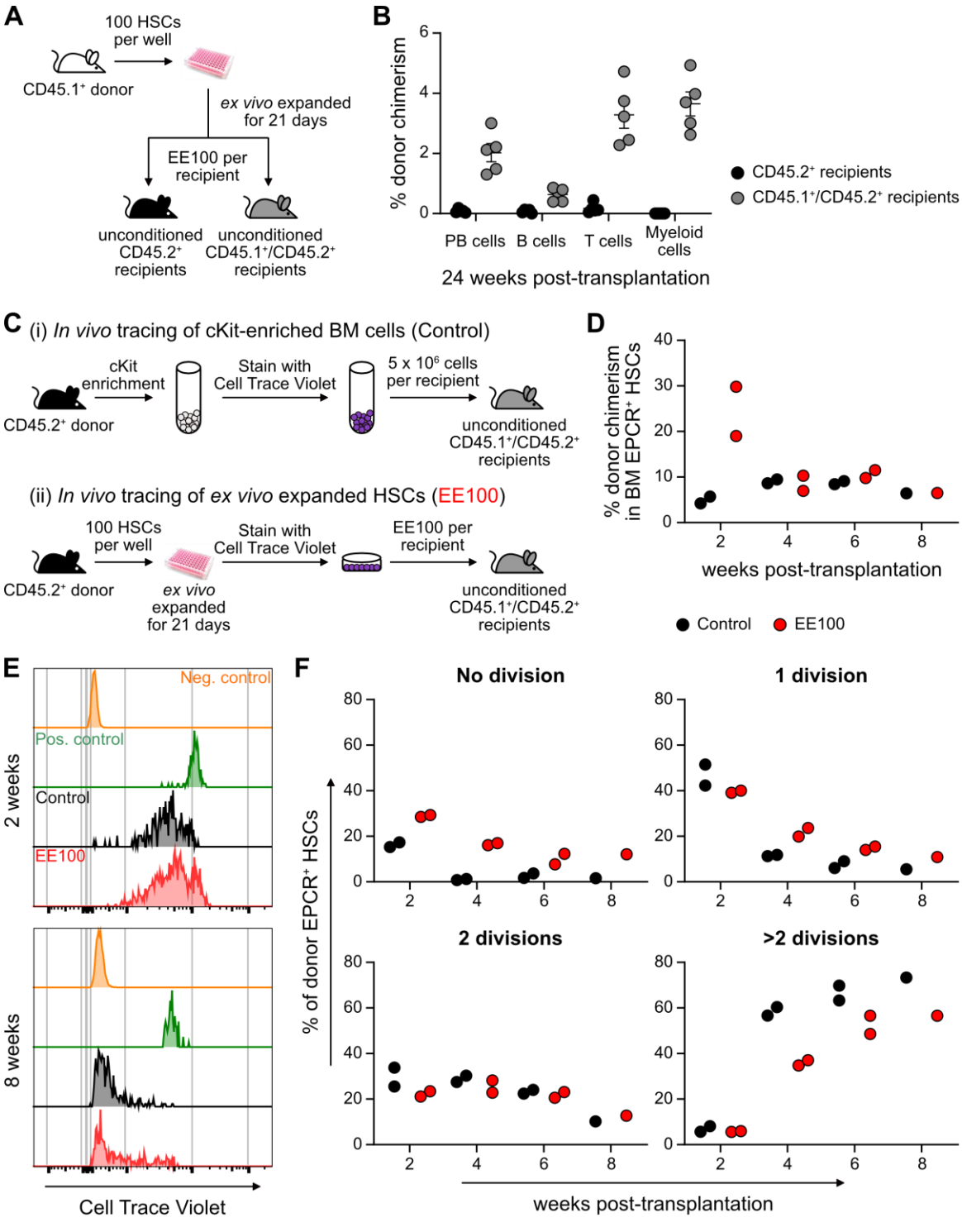

Supplementary Figure 1, Zhang et al.

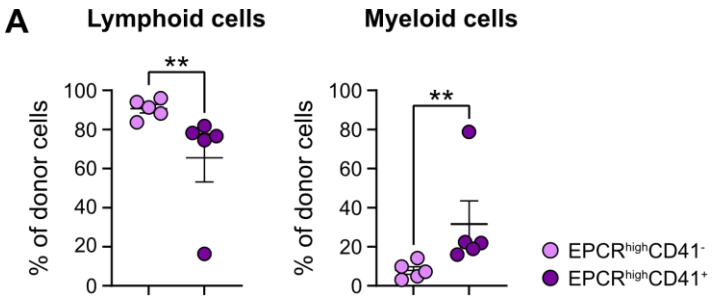

Supplementary Figure 2, Zhang et al.

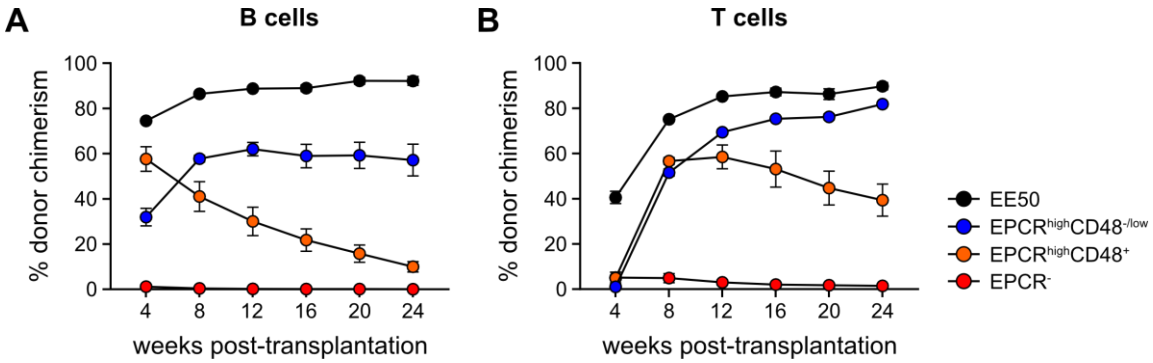

Supplementary Figure 3, Zhang et al.

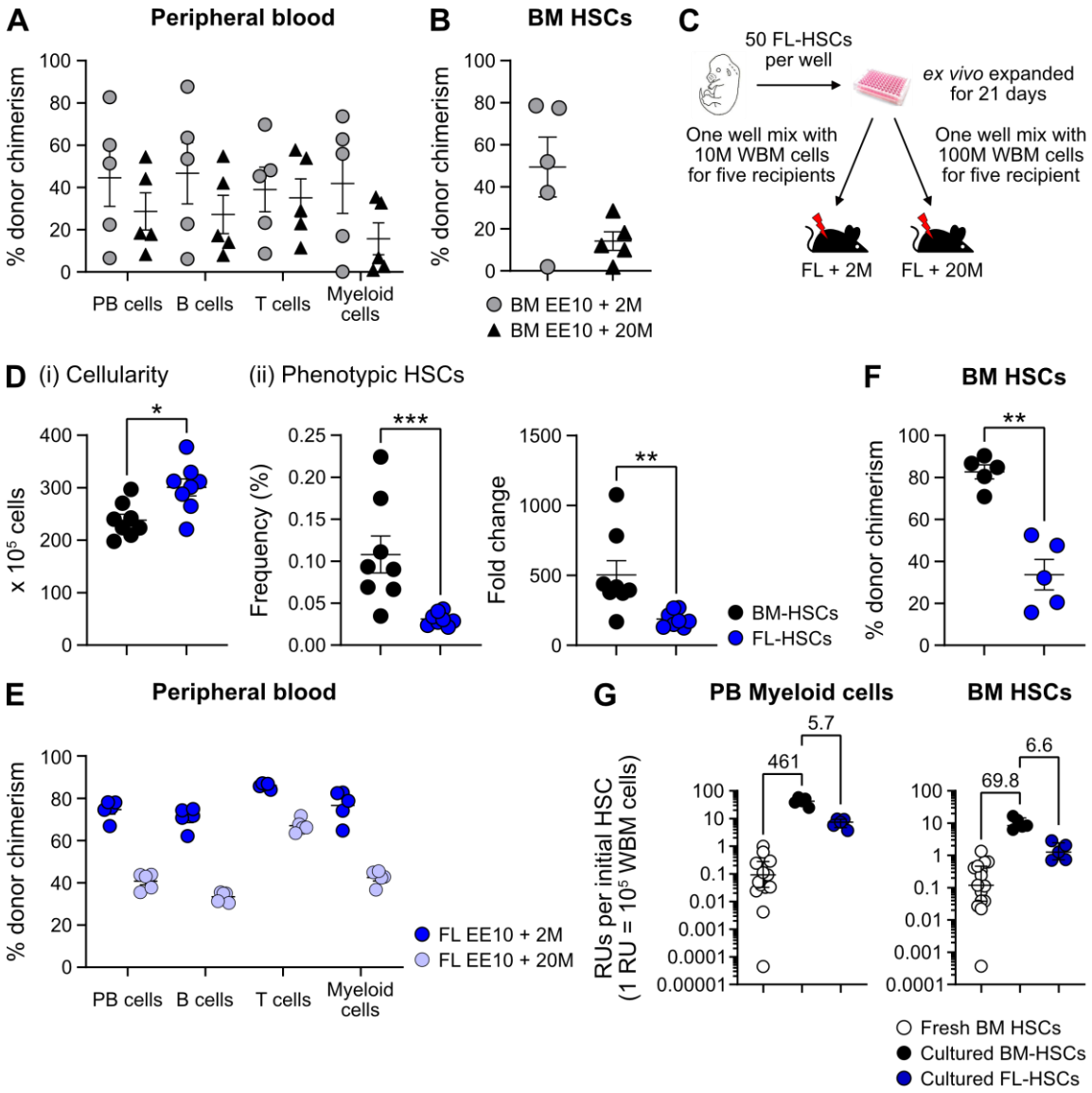

Supplementary Figure 4, Zhang et al.